

## Article

# Indexes for Estimating Outdoor and Indoor Microclimates: A Case Study at the San Panfilo Church in Tornimparte, Italy

Eleonora Racca , Davide Bertoni  and Silvia Ferrarese \* 

Department of Physics, University of Turin, 10125 Turin, Italy; e.racca@unito.it (E.R.);  
davide.bertoni@unito.it (D.B.)

\* Correspondence: silvia.ferrarese@unito.it

**Abstract:** In this work, we consider the indoor and outdoor microclimatic conditions and the influence of the building on their relationship. Microclimatic indexes are a useful tool to characterize microclimatic environments, and they can be used to compare indoor and outdoor microclimate conditions and to evaluate the influence of the building itself on the microclimate. The case study refers to the ancient building of San Panfilo church in Tornimparte (Italy), preserving an important cycle of frescoes by depicted by Saturnino Gatti from 1491 to 1494. The microclimatic conditions were measured during a dedicated campaign at several sites in the church and two sites outside: one in a near-building position and one in an open-air site. In order to characterize the indoor and outdoor microclimatic conditions, some statistical indexes were applied. The results show the comparison in microclimatic conditions in the different sites in the church and between indoor and outdoor environments, allowing for the detection of the influence of the building in the microclimatic conditions.

**Keywords:** microclimate; cultural heritage; indoor environment; outdoor environment; microclimatic indexes



**Citation:** Racca, E.; Bertoni, D.; Ferrarese, S. Indexes for Estimating Outdoor and Indoor Microclimates: A Case Study at the San Panfilo Church in Tornimparte, Italy. *Heritage* **2024**, *7*, 6729–6748. <https://doi.org/10.3390/heritage7120311>

Academic Editor: David Thickett

Received: 13 September 2024

Revised: 13 November 2024

Accepted: 22 November 2024

Published: 28 November 2024



**Copyright:** © 2024 by the authors. Licensee MDPI, Basel, Switzerland. This article is an open access article distributed under the terms and conditions of the Creative Commons Attribution (CC BY) license (<https://creativecommons.org/licenses/by/4.0/>).

## 1. Introduction

Works of art can be preserved over time only if the surrounding microclimate is favorable; in fact, some ancient objects have been preserved for centuries in exceptional conservation conditions, while others have been irretrievably lost. In the first case, works of art have been conserved in favorable microclimatic conditions that delayed degradation phenomena and allowed conservation to continue for centuries; in the second, the microclimate conditions accelerated the degradation processes, and the works of art were completely damaged [1,2].

Works of art can be conserved or exposed to indoor or outdoor conditions. The objects that are hosted inside buildings, for example in libraries, museums, and churches, usually experience more favorable conditions for conservation as a consequence of the physical characteristics of the building itself, such as their thermal capacity and their absorbing power, which can mitigate the fluctuations in temperature and relative humidity. The comparison between outdoor and indoor environmental conditions has been investigated through several studies concerning religious buildings, like churches (e.g., [3–9]) or monasteries (e.g., [10]), historical museums (e.g., [9,11]), and historical libraries (e.g., [12]). The outdoor environment depends on climatic and meteorological conditions, while indoor environments are influenced by outdoor conditions and also by internal sources like the presence of people (e.g., [13]) and by heating or cooling systems (e.g., [14]) that can increase or mitigate fluctuations.

The main method to detect microclimatic conditions is through monitoring activity. In the last thirty years, monitoring activity in historic buildings has been developed with the aim of investigating the microclimate conditions [15]. Monitoring activity is performed by

measuring the microclimatic parameters, mainly temperature, relative humidity, radiation, and the concentration of pollutants. The monitoring activity should be performed for almost one year at the frequency of one datum every 10 or 15 min. The measured values make it possible to evaluate trends and fluctuations to characterize the microclimatic conditions and to individuate potential critical conditions.

Since the 1990s, some standards have been proposed in order to identify the favorable microclimate conditions for the conservation of artworks. The Italian standard UNI10829 [16] defines the safe ranges of temperature, relative humidity, illuminance, UV radiation, and their daily excursions for specific categories of organic and inorganic objects. However, there is no general criterion for the definition of the allowed ranges, as sometimes the safe ranges are defined by the experience of the exhibit curators. The European standard EN15757 [17] was introduced with the aim to overcome this issue, it does not define a list of suggested ranges, but it considers the environmental conditions, where the work of art is acclimatized (historical climate).

Some authors have used the safe ranges proposed by the UNI10829 or values suggested by curators to define some microclimatic indexes useful for classifying microclimatic conditions [18]. Corgnati et al. [19,20] defined the Performance Index (*PI*) as the percentage of time in which the measured parameter lies within the required range. The *PI* was applied simultaneously to temperature and relative humidity at some datasets that were collected in indoor environments during a temporary exhibition in a museum [19,20] and in the monumental complex of Santa Maria della Scala in Siena [21]. The *PI* index was also applied to compare summer and winter conditions in the historical library of Classense Library in Ravenna (Italy) [12], and more recently, it was used to study the microclimate conditions of three museums in Poland [22] and the Milan Cathedral (Italy) [23].

In order to take into account a wider set of parameters, Schito et al. [24] added to the *PI* index four other indexes. They were referred to as the following: (a) a wider range of temperature and relative humidity, (b) illuminance, (c) maximum value in temperature and relative humidity, and (d) spatial homogeneity; they were applied to a monitoring campaign in the Palazzo Blu museum in Pisa. Sciarpi et al. [11] also applied the *PI* index to the daily gradients of temperature and relative humidity to evaluate the variability of these quantities, as suggested in the standards. The case study was an experimental campaign performed inside the Natural History Museum of Florence.

The Index of Microclimatic Excursion (*IME*) considers the daily excursions in temperature and humidity and the number of days when the thresholds suggested by the standard are exceeded for both parameters, or only for one of them, or for none [25]. It can be used in different contexts; for example, it was applied in comparing the microclimatic conditions of some museum showcases [25] and in the rooms of a historical complex (Santa Maria della Carità church in Venice) [26]. Recently, Ferrarese et al. [27] proposed the Index of Microclimatic Variability (*IMV*), which is independent of the thresholds suggested by the standards or by the experience of museum curators.

The Normalized Diurnal Range (*NDR*) and the Relative Humidity ratio ( $RH_{ratio}$ ) indexes can be used to investigate the relationships between indoor and outdoor microclimatic conditions. In particular, both of them give information about the buffering action of the envelope, the room ventilation, and its use [28,29].

The *NDR* is based on the comparison between the diurnal ranges of temperature indoors and outdoors. It was defined in [28] to expand the temperature dataset of the measurements taken in Bologna during the seventeenth century. Later, Verticchio et al. [29] used it to evaluate the buffering capacity of the building in three historic Italian libraries: the Ca' Granda Library in Milan, the Delfiniana Library in Udine, and the CREA Meteorological Library at the Collegio Romano in Rome.

The  $RH_{ratio}$  was defined by Verticchio et al. in [29] to evaluate the effects of moisture and its exchanges between the air and the collections in the libraries of Milan, Udine, and Rome. To do so, the  $RH_{ratio}$  compares the seasonal spreads of humidity measured indoors and outdoors.

The comparison between the number of condensation and evaporation cycles as a function of the micropore radius gives information about the absorption of water in wall micropores [1] and can be used to detect possible deterioration caused by condensation–evaporation cycles. It was first used by Camuffo et al. in [30] to evaluate the deterioration of the Leaning Tower of Pisa (Italy) caused by the cycles in the micropores. Later, it was used by Camuffo et al. in [31] to investigate possible causes of the deterioration of stones, mosaics, and plasters in the Basilica of Santa Maria Maggiore in Rome (Italy) and by Bernardi et al. in [32] to compare the surfaces condensation risk before and after the installation of air drier and air humidifier devices in St. Stephan’s church in Nessebar (Bulgaria).

The indoor microclimate depends on the outdoor meteorological conditions, the internal sources, and the building structure. In this work, we want to compare the indoor measured microclimate with the outdoor and the near-building conditions to evaluate the building influence on indoor microclimate itself by applying the mentioned statistical indexes.

We consider the ancient building of the parish church of San Panfilo in Tornimparte, province of L’Aquila, Italy. The church is of great historical and artistic interest, as it preserves an important cycle of frescoes by Saturnino Gatti (1494). An archaeometric study was conducted by the members of the Italian Association of Archaeometry (AIAR) applying innovative diagnostic techniques in order to study the conservative conditions of frescoes. The whole study describing the pre-restoration conditions of the church and the frescoes had the aim to support the planning of restoration works [33–43]. A dedicated microclimatic monitoring campaign was performed in the context of the project from February 2021 to April 2022 [39].

The complex of S. Panfilo is an isolated building, as it is surrounded by the road and undeveloped land. The ancient and thick walls of the church mitigate the outdoor conditions, resulting in a different indoor climate. Thus, the site is suitable for studying the difference between indoor, near-building, and outdoor conditions considering the measured microclimatic parameters and applying the statistical indexes in the literature. In particular, the  $PI$ ,  $IME$ ,  $IMV$ ,  $NDR$ ,  $RH_{ratio}$ , and the number of condensation and evaporation cycles were computed and discussed in order to evaluate the influence of the building on the microclimatic conditions.

## 2. Materials and Methods

### 2.1. The Site

San Panfilo Church (Figure 1a) is located in central Italy, in the province of L’Aquila, in the municipality of Tornimparte, Villagrande village (latitude:  $42.28864^{\circ}$  N, longitude:  $13.30136^{\circ}$  E), at the altitude of 830 m above sea level (Figure 1b).

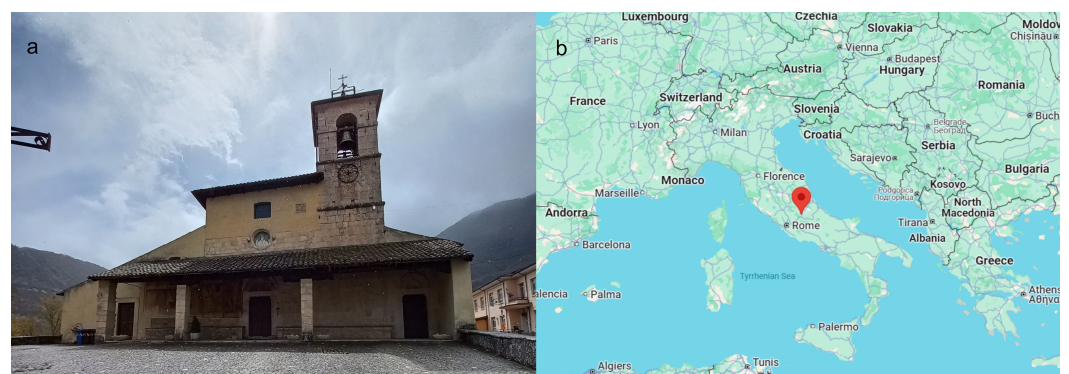


**Figure 1.** Photograph of San Panfilo Church (a) and the geographical position of the municipality of Tornimparte in central Italy (b).

The church has a long history, as it was founded around the year 1000, and its fame is mainly due to the cycle decorating the apse by the painter Saturnino Gatti (1463–1518). The historical context of the church and its frescoes can be found in the archaeometric study that was the subject of a research project conducted by members of the AIAR association [33].

The building includes the church, the rectory, and a wide lateral chapel. The facade with a portico faces the churchyard, which is surrounded by walls.

A microclimatic monitoring campaign was organized in the period from February 2021 to April 2022 with several measurement sites inside the church: one outside the church under the external portico and one at the meteorological station of Colle San Vito (latitude: 42.290639° N, longitude: 13.289556° E) managed by the Centro Funzionale and Ufficio Idrografico of Regione Abruzzo. The Colle San Vito station is located at a distance of about 1 km west of the San Panfilo Church (Figure 2).

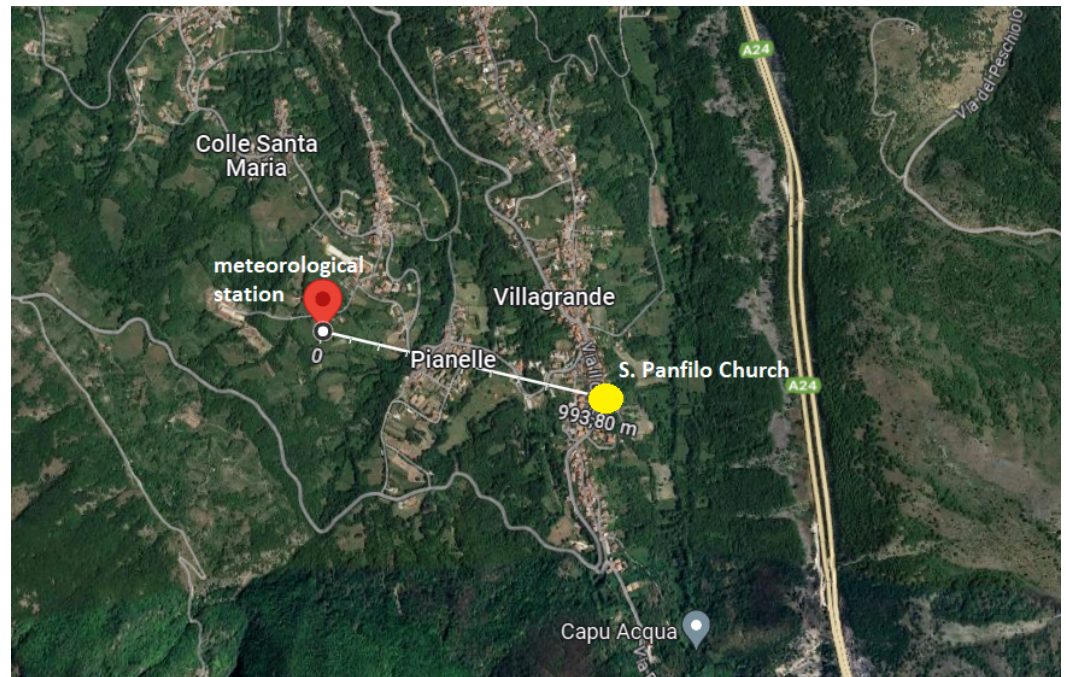


**Figure 2.** Geographical position of Colle San Vito meteorological station (red point) and San Panfilo Church (yellow point).

## 2.2. The Measurements

The microclimatic campaign included intensive monitoring activity during some specific days and continuous monitoring at some sites during the monitoring period. The sensors were located at two different levels above the floor at about 1 m and 2.5 m. The data were collected by several thermo-hygrometers HOB0-UX100-011 manufactured by Onset, working at a frequency of 1 datum every 10 min. The accuracy for temperature was 0.21 °C, the resolution was 0.024 °C, and the measurements could range between −20 °C and 70 °C. For the relative humidity, the accuracy was 2.5%, the resolution was 0.05%, and the range was between 1% and 95%. The details of the monitoring campaign are described in [39]. In the present work, the data collected at eight positions inside the church are considered to characterize the indoor microclimate. In contrast, the near-building microclimate was detected by the sensor under the portico (Table 1; see Figure 3). The outdoor meteorological conditions were measured at the station of Colle S. Vito (Figure 2) at the frequency of 1 datum every 15 min.

The monitoring campaign was conducted between February 2021 and April 2022; however, in order to compute the indices in a balanced way, it was decided to limit the data to a year, and the selected period was between 1 March 2021 and 28 February 2022. The church can be heated through several fan coils. However, during the measurements, they were switched off due to countermeasures against the COVID-19 pandemic. The lighting system consists of a number of LED lights over the column capitals, and its contribution to heating is negligible. For these reasons, during the measurement period, the sources of heat were the presence of people, who usually only enter the church during Sunday masses and religious holidays, and the natural lighting through the windows. The

absence of artificial heating permits the investigation of the building capacity in the case of unperturbed conditions.

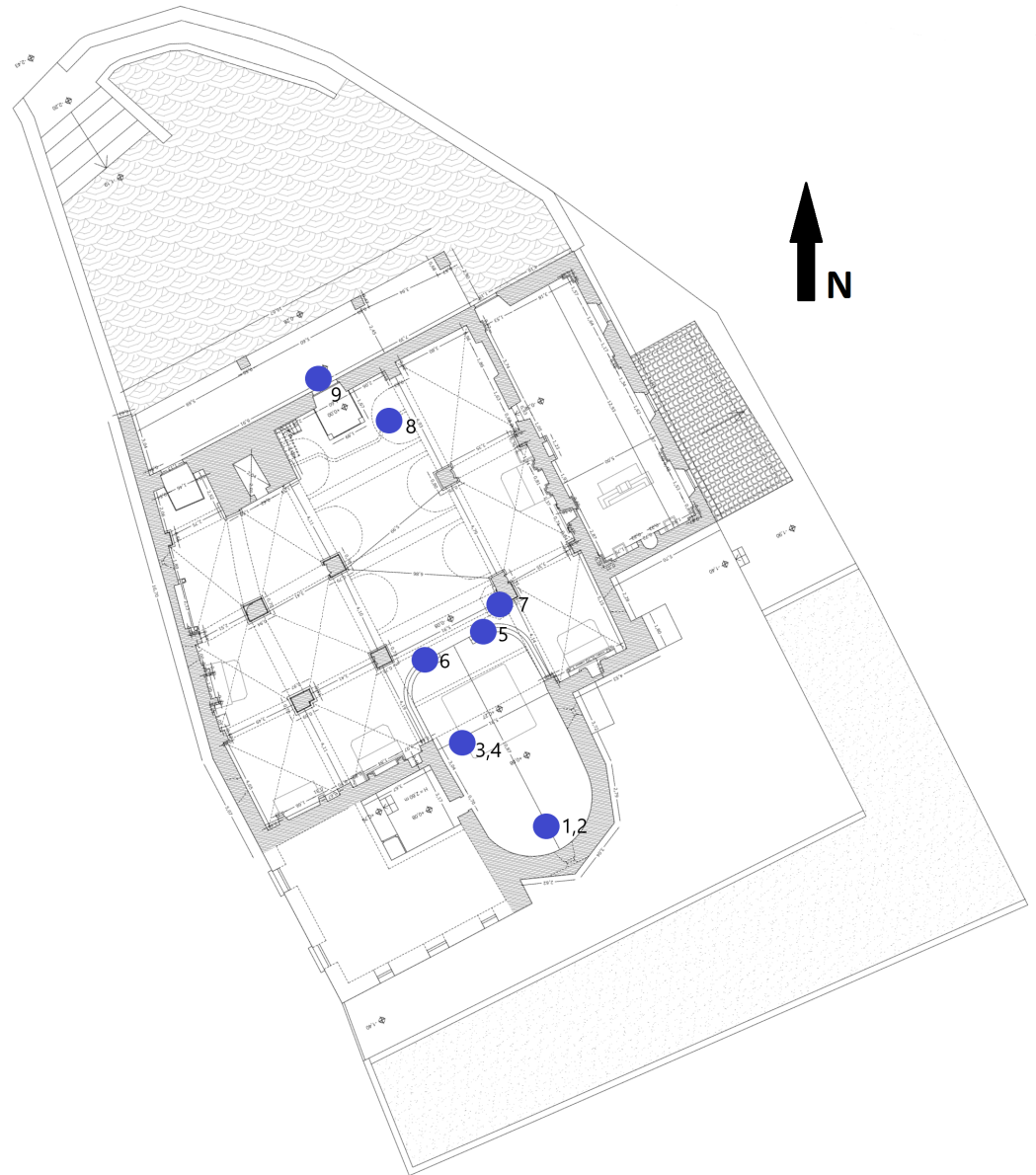


**Figure 3.** Church plan with the positions of thermo-hygrometers (blue points) installed inside the church and under the external portico.

**Table 1.** Positions and heights of the indoor sensors of the monitoring campaign included in this analysis.

Ref. in Figure 3	Location	Height Above Floor (m)
1	Case (left)	0.86
2	Case (right)	0.86
3	Crucifix (bottom)	1.10
4	Crucifix (top)	2.07
5	Balustrade (left)	0.56
6	Balustrade (right)	0.56
7	Pulpit	2.14
8	Choir	2.78
9	Portico	2.68

### 2.3. Microclimatic Indexes

The microclimatic indexes included in this analysis are detailed below.

The first microclimatic index applied to the dataset of this measurement campaign was the *PI* index. This index was developed by Corgnati et al. [19,20] in the context of a proposal for a procedure to assess the indoor environmental quality in the presence of HVAC (Heating, Ventilating, and Air Conditioning) systems. It is defined as the percentage of the time during which the measure of the parameters lie in a fixed range for the total duration of the measuring campaign:

$$PI = 100 \cdot \frac{t_{in}}{t_{tot}}, \quad (1)$$

where  $t_{in}$  is the time when the measure is in the range, and  $t_{tot}$  is the total duration. The original *PI* proposed in [19], considered only one parameter at a time, while the extension developed in [20] considered temperature and relative humidity simultaneously. The *PI* index evaluates how well the building performs when trying to maintain temperature and relative humidity in a defined range suggested by the exhibition curators. It ranges between 0% for low performances and 100% if all measurements are included in the suggested ranges of temperature and relative humidity. Therefore, its values correspond to classes of indoor air quality assessment: class A buildings have *PI* values higher than 90%, class B buildings have *PI* values from 85% to 90%, class C buildings have *PI* values from 80% to 85%, and finally, lower values are for not classified buildings.

Another microclimatic index applied is the *IME*, developed by Ferrarese et al. in [25]. The index accounts for the daily excursions of temperature and relative humidity and their daily limits given by UNI10829 [16]. It is defined as follows:

$$IME = \frac{n_1 - n_3}{n_{tot}} + \frac{n_2 + n_4}{2n_{tot}}, \quad (2)$$

where  $n_1$  is the number of days when the limits are respected,  $n_3$  the number of days exceeding the limits on both temperature and relative humidity, and  $n_2$  and  $n_4$  are the number of days during which one between the excursions of temperature or relative humidity exceeds the limits; finally,  $n_{tot}$  is the total number of days of the campaign. The index can be evaluated on yearly sets of data. It ranges between  $-1$ —if all measures exceed the threshold values—and  $1$ —when the excursions are within the limits.

The *IMV* index is an improvement of the *IME* index developed by Ferrarese et al. in [27]. This improvement was motivated by the usage of suggested thresholds: the evaluation of the *IME* is dependent on the thresholds given by the UNI10829 [16] or can easily be adapted with different thresholds, which are decided by museum curators. However, a general criterion to establish whether a condition is critical for any type of artwork is yet to be defined. In order to overcome the usage of the thresholds, the *IMV* computes the maximum daily excursion of temperature and relative humidity and weights them through a Gaussian relationship:

$$IMV = \frac{\sum_{d=1}^{n_{days}} \left[ 2 \exp\left(\frac{\Delta_d^2}{2a^2}\right) - 1 \right]}{n_{days}} \quad (3)$$

where  $n_{days}$  is the number of days of the campaign,  $\Delta_d$  is the information on the variability of temperature and relative humidity during each day, and  $a$  is the parameter that amplifies the differences between *IMV* indexes and in this analysis is 30, as defined in [27]. *IMV*, as *IME*, varies between  $-1$ , the worst condition, and  $1$ , which is the best possible evaluation.

The *NDR* index can be used to investigate the buffering capacity of the building structure and envelope to limit the external excursions of temperature. It was defined in [28] through the following equation:

$$NDR = \frac{\sum_{n=1}^{n_{SP}} \frac{(T_{n,14} - T_{n,22})_{SP}}{n_{SP}}}{\sum_{n=1}^{n_{RP}} \frac{(T_{n,14} - T_{n,22})_{RP}}{n_{RP}}} \quad (4)$$

where  $T_{n,14}$  is the measure at 14:00 of the  $n^{th}$  day and the closest to the daily maximum;  $T_{n,22}$  is the  $n^{th}$  day temperature at 22:00 and the closest to the daily average;  $n_{SP}$  is the number of days of the selected period;  $n_{RP}$  are the days in the reference period.  $T_{n,14} - T_{n,22}$  represents half of the daily range of temperatures, which has a seasonal behavior. The normalization eliminates the seasonality and compares the indoor daily excursions (SPs) to those outdoors (RPs). When *NDR* is zero, the building has a large buffering capacity and limited ventilation. *NDR* is maximum when it equals one; the temperatures are the same as those outside, and the room is greatly ventilated.

In this article, it was decided to modify Equation (4) as follows:

$$NDR = \frac{n_{outdoor}}{n_{indoor}} \cdot \frac{\sum_{n=1}^{n_{indoor}} \Delta T_{n,indoor}}{\sum_{n=1}^{n_{indoor}} \Delta T_{n,outdoor}} \quad (5)$$

where  $\Delta T_n$  is the  $n^{th}$  daily half-excursion, and  $n_{indoor}$  and  $n_{outdoor}$  are the number of days of the measurement taken indoors and outdoors, respectively. In the original equation, the difference between two temperatures represents half of the daily range; however, in this measuring campaign, the data are taken every 10 min, and therefore, they are more representative of the daily behavior. For this reason, it was decided that half of the daily excursion should be taken into account directly, without estimating the highest temperature and the one closer to the average for each day.

The  $RH_{ratio}$  was defined to study the possible effects of the moisture exchanges by [29] through this equation:

$$RH_{ratio} = 100 \cdot \frac{\sum_{i=1}^m |RH_{i,90d} - RH_i|_{indoor}}{\sum_{i=1}^m |RH_{i,90d} - RH_i|_{outdoor}} \quad (6)$$

where  $RH_{i,90d}$  is the  $i^{th}$  centered moving average for 90 days of relative humidity,  $RH_i$  is the  $i$ -th measure of relative humidity, and  $m$  is the total number of measures. Therefore, the  $RH_{ratio}$  is the percentage ratio between the seasonal spreads of indoor and outdoor relative humidity. If it is close to zero, there are limited air exchanges between indoors and outdoors; when it is close to 100, the building has no effects, as the excursions are the same. In this measuring campaign, the indoor sensor took measurements every 10 min, while the data from the meteorological station were measured every 15 min. For this reason, it was decided to modify Equation (6) by introducing the number of measures:

$$RH_{ratio} = 100 \cdot \frac{m_{outdoor}}{m_{indoor}} \cdot \frac{\sum_{i=1}^{m_{indoor}} |RH_{i,90d} - RH_i|_{indoor}}{\sum_{i=1}^{m_{outdoor}} |RH_{i,90d} - RH_i|_{outdoor}} \quad (7)$$

where  $m_{indoor}$  and  $m_{outdoor}$  are the number of measures taken, respectively, indoors and outdoors. The normalization is necessary to account for the different number of measurements.

It was also decided that the daily saturation of the micropores should be evaluated, which is caused by the daily cycles of condensation and evaporation due to the Kelvin effect [44]. The radii of the micropores analyzed range was between  $1.0 \times 10^{-9}$  m and  $1.0 \times 10^{-6}$  m. The number of days during which the micropores were always, sometimes, or never saturated, which was calculated for each radius. To do so, for all the measurements taken every 10 or 15 min, the correspondent critical relative humidity values were evaluated through this equation [1]:

$$RH_c = 100 \cdot \exp\left(\frac{2\sigma V_m}{rRT}\right), \quad (8)$$

where  $\sigma = 0.0756 \text{ N m}^{-1}$  is the surface tension of water,  $V_m = 1.8 \times 10^{-5} \text{ m}^3 \text{ mol}^{-1}$  is the molar volume of water,  $r$  is the negative radius of the micropore in meters [1],  $R = 8.314510 \text{ J mol}^{-1} \text{ K}^{-1}$  is the ideal gas constant, and  $T$  is the ambient temperature in kelvin. When the measured relative humidity exceeds the critical relative humidity, the micropore of radius  $r$  is saturated; otherwise, it is not.

The pores can be classified as always filled with water, never filled with water, or submitted to evaporation and condensation cycles. The smaller pores are always full of water; they are a water reservoir for microbiological life and for the freezing in the greatest pores after absorption from smaller pores. The pores submitted to evaporation and condensation cycles are at risk of dissolution and recrystallization of salt that causes salt migration and efflorescence [30]. In order to compare the different critical radii distribution, we have considered the minimum never-filled radius.

### 3. Microclimatic Data

In this section, the measures of the temperature and relative humidity taken during the monitoring campaign in the period selected between 1 March 2021 and 28 February 2022 are presented. Moreover, the values of specific humidity, dew point temperature, and dew point spread have been computed and are shown.

To efficiently describe the microclimatic conditions, it was decided to compare the behaviors of the measures taken at the pulpit, under the portico, and at the meteorological station. It was decided to consider the pulpit as the representative of indoor sensors because of its central position, as shown in Figure 3. Furthermore, as already analyzed in [39], other sensors in the church present some spikes of temperature and relative humidity, which have a rising time of one hour and which cause variations of up to  $3^\circ\text{C}$  and up to 12%, respectively. These spikes can be observed in the data of the sensors placed on the case, near the choir, and on the balustrade on the left. Their timing suggests that a possible cause is the presence of direct radiation on the surfaces from the central window in the apse and from lateral windows in the main nave [39]. In the presence of spikes, the time series are not representative of the whole microclimate of the church, but only of the sites where the measurements were performed. Nevertheless, these measurements show that the surfaces exposed to direct radiation are subjected to an increase in temperature. On the contrary, at the pulpit site, direct sunlight did not impact the sensor, and its time series does not present temperature or relative humidity spikes, so they can be considered representative of the indoor microclimate. The measurements under the portico are representative of the near-building conditions, while those at the meteorological station represent outdoor open-air conditions. Measured data near the pulpit, under the external portico, and at the meteorological station in the pictures are usually represented in red, green, and blue respectively.

Figure 4 shows the data of the temperature and relative humidity taken in the selected period for two of the sensors, which were placed at the pulpit and under the portico outside the church, as well as those taken at the meteorological station of Colle S. Vito.



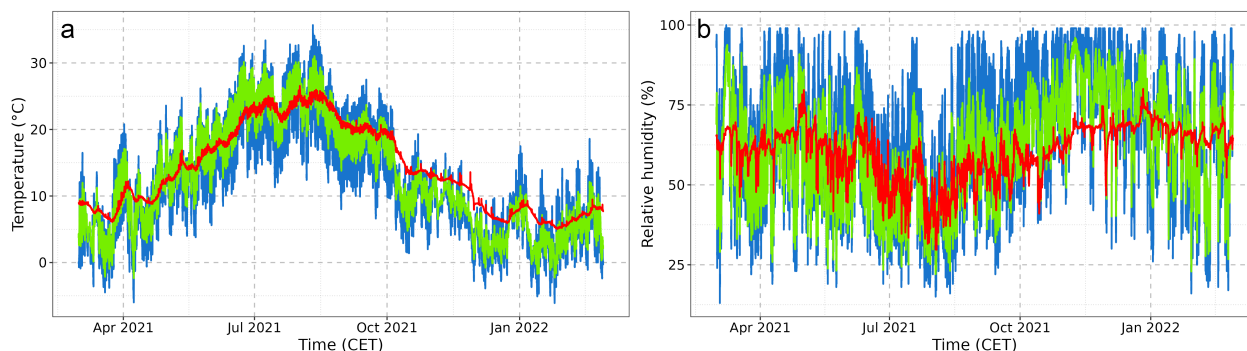


**Figure 4.** Measures of temperature (a) and relative humidity (b) of the sensors located in pulpit (red), portico (green), and meteorological station (blue).

The values show that the temperature (in Figure 4a) is modulated by the season, meteorological events, and the day–night rhythm. The seasonality is noticeable in the thermal wave, with higher values in summer and lower values in winter; the meteorological events add the fluctuations with a time scale of 2–7 days, while the fastest fluctuations are due to the day–night rhythm. Under the external portico, the influence of the building is recognizable in the fluctuations in temperature, which have lower amplitude values compared to the recorded values at the meteorological station. Inside the church, the thermal capacity of the thick walls further limits the fluctuations and mitigates the winter lower and the summer higher temperatures; moreover, it introduces a time delay. The relative humidity values (in Figure 4b) depend on the meteorological events and show the influence of the building in limiting the fluctuations, both in the measurements of the portico and the pulpit.

These considerations are highlighted in Figure 5, showing the daily excursions and the monthly moving averages in temperature and relative humidity. In particular, the moving averages show clearly the seasonal behavior of the microclimatic quantities. The average temperature inside the church is always higher than under the portico except for the period between May and July, as can be expected in ancient buildings with thick walls [31].

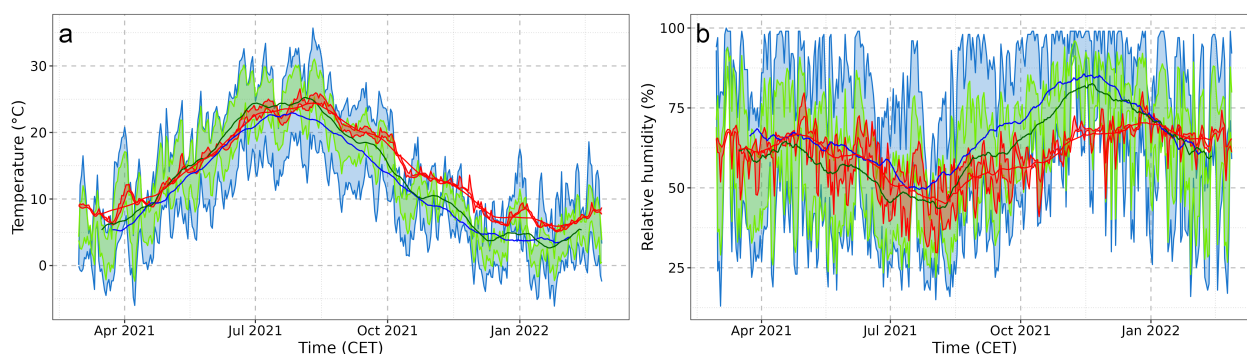


**Figure 5.** Daily excursions and monthly moving average of temperature (a) and relative humidity (b) of the sensors located in pulpit (red), portico (green), and meteorological station (blue).

Observing the graphs in Figure 4, a delay in the behavior of the temperature can be seen when comparing outdoor and indoor conditions. The delay can be estimated through the cross-correlation analysis of the measures taken at the pulpit, under the portico, and at the meteorological station. The results are summarized in Table 2 along with the computed correlation.

The smallest delay can be observed in the correlation between the portico and the meteorological station. Indeed, the building introduces a delay of only two hours, due to the boundary layer conditions in the near-building microclimate. In order to better show the delay between the measures at the meteorological station and at the portico, in Figure 6a, their values are depicted during three days in July.

A greater effect of the buffering capacity of the building on the microclimate can be observed indoors. The cross-correlation analysis reveals a delay of three days considering both the correlation between the portico and the pulpit and when comparing the pulpit and the meteorological station. A delay of three days between indoors and outdoors was also reported in [39], where the reference for the measurements inside the church is the sensor placed at the top of the crucifix. As an example, Figure 6b shows the daily averages temperature during the months of March and April 2021, where the delay of three days between indoors and outdoors is recognizable.

**Table 2.** Temporal delay between the measurements taken indoors and outdoors.

Locations	Delay lag	Correlation
Pulpit—Portico	3 d	0.97
Pulpit—Meteorological station	3 d	0.94
Portico—Meteorological station	120 min	0.97

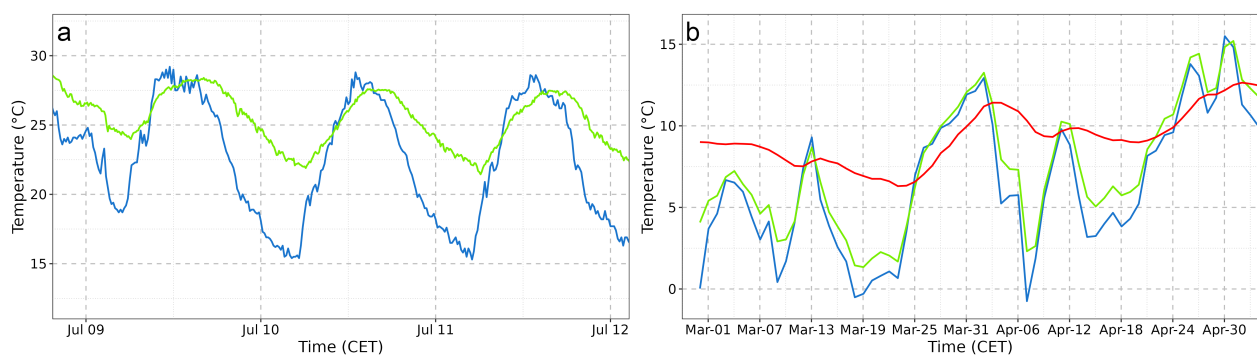


**Figure 6.** Measures of temperature under the portico (green) and at the meteorological station (blue) between 9 July and 12 July 2021 (a). Daily averages of temperature at the pulpit site (red), under the portico (green), and at the meteorological station (blue) during March and April 2021 (b).

In Figure 7, the graphs of dew point temperature and specific humidity are depicted. The dew point (Figure 7a) is the temperature at which a parcel of moist air should be cooled to obtain saturation at constant atmospheric pressure and water vapor content. It was evaluated using the following relation:

$$T_d = b \frac{aT + (b + T) \cdot \log\left(\frac{RH}{100}\right)}{ab - (b + T) \cdot \log\left(\frac{RH}{100}\right)} \quad (9)$$

where  $a = 7.5$  and  $b = 237.3^\circ\text{C}$  are the coefficients of Magnus and Tetens for vapor in equilibrium with the liquid phase [1],  $T$  is the ambient temperature measured in celsius, and  $RH$  is the relative humidity.

The specific humidity (Figure 7b) is the ratio between the masses of water vapour and moist air. It was computed using the following relation:

$$SH = 0.62197 \cdot \frac{e}{p - e} \cdot 100, \quad (10)$$

where  $e$  is the vapor pressure, and  $p$  is the atmospheric pressure at the altitude of Tornimparte.  $e$  is evaluated through the Bolton parametrization [45], as previously done in [39].

$$e = \frac{0.62197 \cdot RH}{100} \exp\left(\frac{17.67 \cdot T}{T + 243.5}\right). \quad (11)$$

In conservation science, it is used to detect the presence of people, window openings, leakages, paths of air masses, and possible evaluation of condensations.

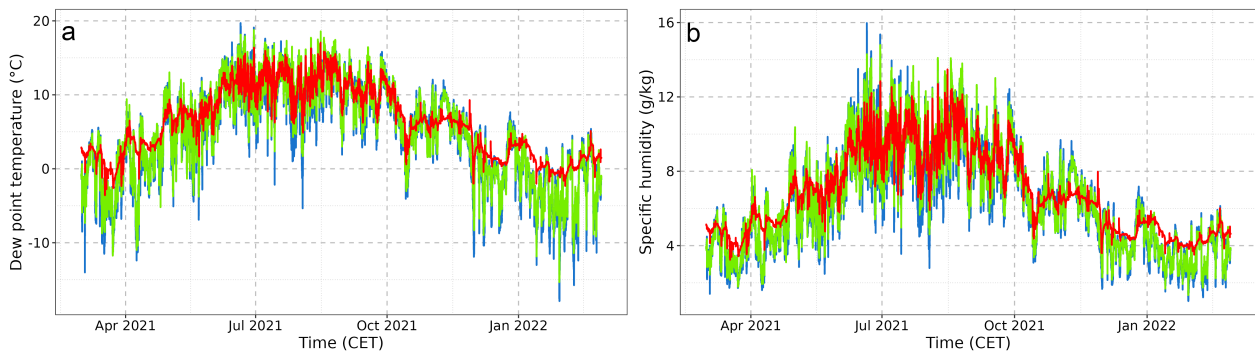


**Figure 7.** Calculated values of dew point temperature (a) and specific humidity (b) of the sensors located in pulpit (red), portico (green), and meteorological station (blue).

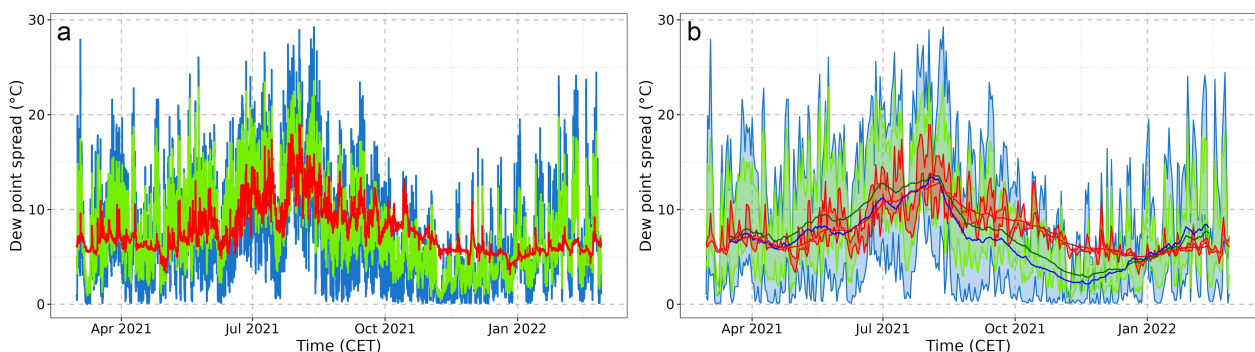
The dew point temperature and specific humidity values (Figure 7) show the expected maxima during the summer and low values in winter as a consequence of seasonality. The time series shows the overlapping of seasonal trends, meteorological events, and in the church, the presence of people during the holy services. The presence of people is recognizable, especially during autumn months at weekly frequency, when temperature, relative humidity (Figure 4), and specific humidity (Figure 7b) present some maxima. It can be observed in the measures taken at the pulpit site that, on average, the temperature increases by about  $1.5^{\circ}\text{C}$ , the relative humidity increases about 5%, and the specific humidity increases by about  $1\text{ g kg}^{-1}$ . The temperature maxima are lower due to the thermal capacity of the walls.

Figure 8a shows the dew point spread, which was evaluated as the difference between the measured temperature and the calculated dew point:

$$\Delta T_d = T - T_d. \quad (12)$$

The dew point spread represents the proximity between the air temperature and the dew point, indicating the possibility of condensation over the surfaces.

The dew point spread values (Figure 8a) were always positive inside the church and under the portico, showing the unlikelihood of condensation over the surfaces. The moving monthly averages (Figure 8b) show a significant difference in the three sites during fall, when indoor averages were higher than near-building and outdoor ones. Nevertheless, at the meteorological station, favorable conditions for condensation can occur, mainly at night. In Table 3, the percentages of events with dew point spreads lower than  $0.2^{\circ}\text{C}$  and  $2^{\circ}\text{C}$  inside the church, under the external portico, and at the meteorological station are shown.



**Figure 8.** Calculated dew point spread (a) and its monthly moving average (b) of the sensors located in pulpit (red), portico (green), and meteorological station (blue).

**Table 3.** Percentages of time during which the dew point spread ( $\Delta T_d$ ) was lower than  $0.2^\circ\text{C}$  and less than  $2^\circ\text{C}$ .

Locations	$\Delta T_d \leq 0.2^\circ\text{C}$	$\Delta T_d \leq 2^\circ\text{C}$
Pulpit	0.00%	0.00%
Portico	0.00%	4.68%
Meteorological station	0.04%	20.56%

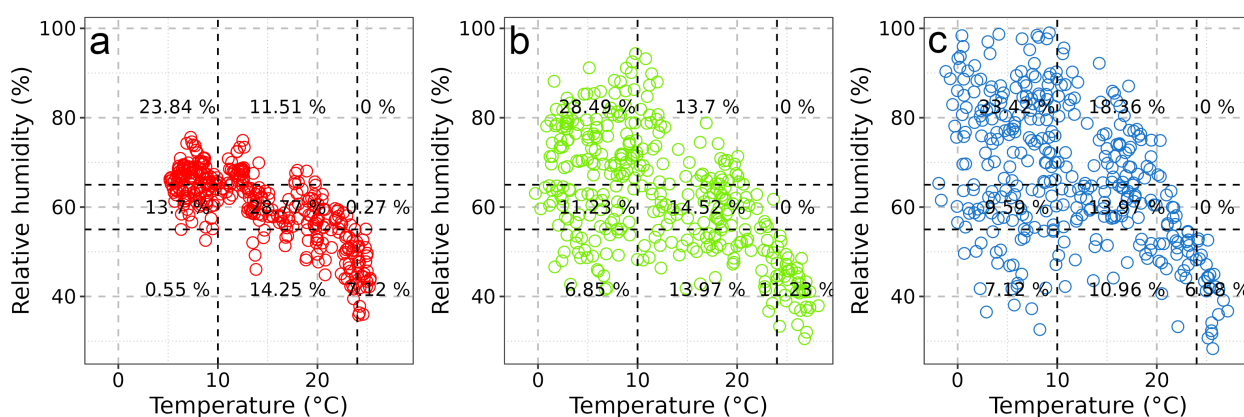
#### 4. Results and Discussion About Microclimatic Indexes

##### 4.1. PI Index

In this case study, the *PI* index defined as in Equation (1) was applied considering the temperature and relative humidity ranges for frescoes defined by the UNI10829 [16]. According to this standard, the temperature should range from  $10^\circ\text{C}$  to  $24^\circ\text{C}$ , and the relative humidity should range from 55% to 65% for frescoes.

Figure 9 depicts the scatter plots of the daily average temperatures and relative humidities for the measurements taken at the pulpit, under the portico, and at the meteorological station. The dotted lines were included to highlight the acceptable ranges of the microclimatic variables defined by the UNI10829 [16]. Each plane is divided into nine squares, where the percentages of data occurrences are written: the *PI* index is the percentage-reported central square. Table 4 summarizes the *PI* indexes of all the sensors included in the analysis and the days during which the measurements lie in the ranges of optimal conditions for fresco preservation.

All the indoor sensors present a behavior similar to the scatter plot in red (Figure 9a), which collects the daily averages of temperature and relative humidity of the sensor at the pulpit. On average, the maximum percentages are included in the central square, where the conditions are optimal for preservation according to the standard. In the top-left square, where the temperature is lower than recommended and the relative humidity presents higher values, slightly lower values of percentages were reached. The green scatter plot (Figure 9b) represents the daily averages of the measures under the portico. In this case, the most frequent condition is represented by higher-than-recommended values of relative humidity and lower temperatures. Comparing these values to indoor conditions, the values tended to be more spread, though not as spread as those registered by the meteorological station (Figure 9c).

**Figure 9.** Daily averages of temperature and relative humidity measured in pulpit (a), portico (b), and meteorological station (c).

Regardless of whether the measures were taken inside or outside the church, based on the values in Table 4, it can be observed that most of the time during the measuring campaign the environmental conditions for the frescoes are not optimal according to the regulations.

**Table 4.** *PI* index evaluated for all sensors placed in the church included in the analysis and at the meteorological station.

Locations	<i>PI</i> (%)
Case (left)	30.68
Case (right)	30.72
Crucifix (bottom)	29.59
Crucifix (top)	29.59
Balustrade (left)	29.04
Balustrade (right)	28.49
Pulpit	28.77
Choir	27.95
Portico	14.52
Meteorological station	13.97

Nevertheless, we can use the *PI* indexes to compare the different sites of measurement inside and outside the church. The values of the *PI* indoors are very close to each other, with values greater than 27%, while the portico and the meteorological station have indexes lower than 15%; therefore, the *PI* index is able to identify indoor and outdoor conditions. However, it seems not to be sensible to different indoor conditions; for example, the presence of spikes on the case, on the balustrade on the left, and at the choir was not detected. Moreover, it seems not able to distinguish between near-building conditions (under the portico) and open-air sites (at the meteorological station).

#### 4.2. *IME and IMV Indexes*

Both the *IME* and the *IMV* indexes were evaluated using, respectively, Equations (2) and (3) to compare their characteristics with a dataset different from the one used to define them.

In the original work [25], the *IME* was defined for archive materials (e.g., manuscripts, printed volumes, and stamps), using thresholds of 1.5 °C for the temperature and 5% for the relative humidity. For the San Panfilo Church, these values were adjusted to 1.5 °C for the temperature and 6% for the relative humidity, as recommended by the UNI10829 for frescoes and paintings, which are present both inside the church and under the portico.

The *IMV* was not adjusted, because it is independent from the thresholds, and it is an index expected to work in comparing microclimatic conditions for different microenvironments.

Figure 10 depicts the scatter plots representing the daily excursions of temperature and relative humidity for the measures taken at the pulpit, the portico, and the meteorological station. The dotted lines represent the thresholds used for temperature and relative humidity to compute the *IME* index. The percentages written in the graphs represent the occurrences of the point in each sector of the plane. The sensors indoors (Figure 10a) present the highest percentages of data in the ranges under the thresholds, followed by several days during which the thresholds for temperature were satisfied, while the relative humidity had variations that were too wide. When outdoors, as can be seen in the data taken under the portico (Figure 10b), the majority of the days for both the temperature and relative humidity excursions exceeded the thresholds, and this behavior was further exacerbated at the meteorological station (Figure 10c).

Table 5 summarizes the calculated *IME* and *IMV* indexes. In the case of the *IMV* index, two of them were evaluated: the first was the  $IMV_{all}$  that accounts for all the sensors, installed both indoors and outdoors, and the  $IMV_{indoor}$ , which takes into account only the indoor sensors. The *IMV* was re-evaluated using only the data of the sensors installed indoors to emphasize better the differences between indoor sites. For the computation of the *IMV* index, the maximum daily excursions of all the considered sensors were needed. In the case of the  $IMV_{all}$ , those used were measured by the meteorological station, while for the  $IMV_{indoor}$ , they were the ones measured by the sensors installed in the choir.

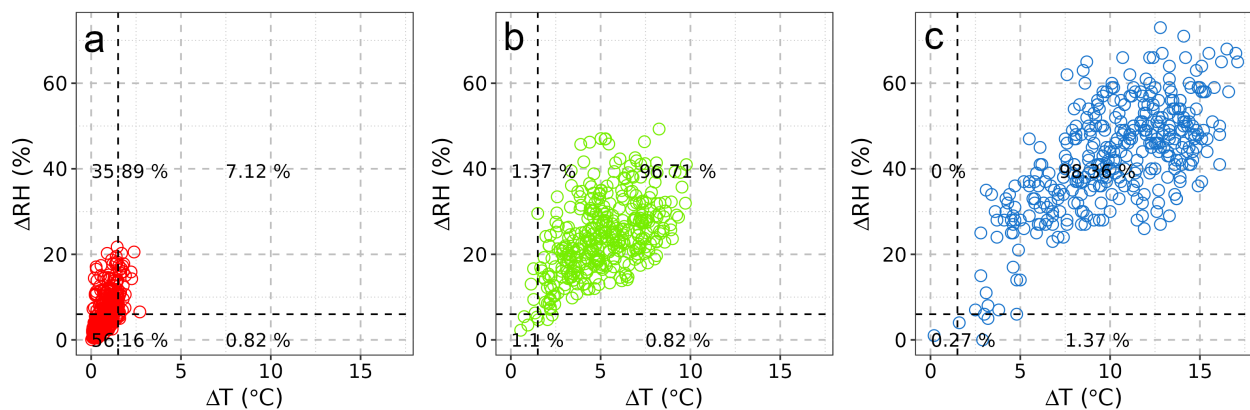


**Figure 10.** Daily excursions of temperature and relative humidity measured in pulpit (a), portico (b), and meteorological station (c).

The *IME* and *IMV* can distinguish between outdoor and indoor conditions and also between different sites inside the church. They use instantaneous values, and therefore, they are influenced by the presence of spikes. It can be observed that the most favorable microclimate conditions are near the pulpit and the crucifix.

**Table 5.** *IME* and *IMV* indexes evaluated for all sensors placed in the church included in the analysis and at the meteorological station.

Locations	<i>IME</i>	<i>IMV</i> <sub>all</sub>	<i>IMV</i> <sub>indoor</sub>
Case (left)	0.44	0.89	0.45
Case (right)	0.48	0.90	0.47
Crucifix (bottom)	0.68	0.92	0.59
Crucifix (top)	0.66	0.92	0.59
Balustrade (left)	0.56	0.92	0.56
Balustrade (right)	0.57	0.91	0.56
Pulpit	0.67	0.93	0.61
Choir	0.57	0.89	0.51
Portico	−0.95	0.13	-
Meteorological station	−0.97	−0.62	-

#### 4.3. *NDR* and *RH<sub>ratio</sub>* Indexes

The *NDR* and *RH<sub>ratio</sub>* indexes were evaluated using, respectively, Equations (5) and (7), and their values were collected in Table 6. In this work, the *RH<sub>ratio</sub>* was computed considering the running average at 90 days and 30 days in order to verify whether there are differences between the seasonal and the monthly behaviors.

From the result of the calculation, both the *NDR* and *RH<sub>ratio</sub>* point out that the building has a great buffering capacity, and there is limited ventilation. Indeed, for indoor sensors, both values are very low. The *NDR* index identified values lower than 0.11 indoors, while under the portico, it was found to be 0.50. The *RH<sub>ratio</sub>* indoor was always lower than 29% and under the portico was greater than 58%.

The *RH<sub>ratio,90d</sub>* values inside the church were higher than the same indexes computed inside historical libraries [29], where the hygroscopic objects limited the fluctuations in relative humidity. San Panfilo Church hosts few hygroscopic objects (the pews, the pulpit, and the balustrade) that can limit the fluctuations in relative humidity.

In summary, the *NDR* and *RH<sub>ratio</sub>* can identify the differences between indoor and outdoor conditions. However, they cannot distinguish between different measurement sites inside the church.

**Table 6.** Evaluated values of  $NDR$  and  $RH_{ratio}$  indexes.

Locations	$NDR$	$RH_{ratio,90\text{ d}}\%$	$RH_{ratio,30\text{ d}}\%$
Case (left)	0.11	27.19	22.93
Case (right)	0.10	28.45	23.99
Crucifix (bottom)	0.07	27.25	22.74
Crucifix (top)	0.08	27.37	22.80
Balustrade (left)	0.08	27.26	22.54
Balustrade (right)	0.08	27.94	23.21
Pulpit	0.07	26.79	22.21
Choir	0.10	25.84	21.58
Portico	0.50	61.58	58.95
Meteorological station	1.00	100	100

#### 4.4. Minimum Radius of Unfilled Micropores

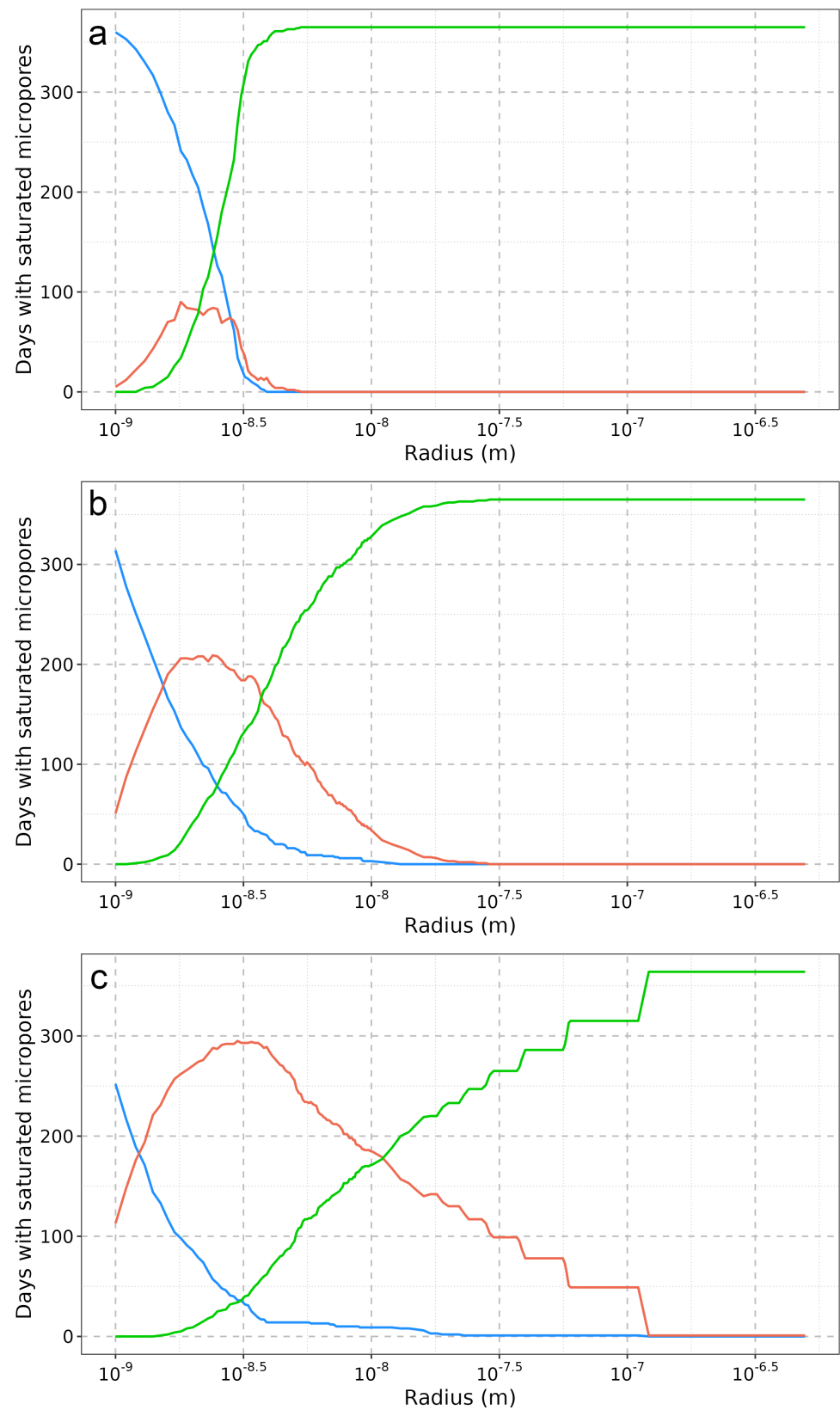
Using Equation (8), the values of critical relative humidity  $RH_c$  for each sensor and for the radii of micropores in the range between  $1.0 \times 10^{-9}$  m and  $1.0 \times 10^{-6}$  m were evaluated. Then, each  $RH_c$  was compared with the relative humidity measures; when the latter is greater, the micropore is considered saturated. After that, the daily saturation was considered, and the results are depicted in Figure 11. In the Figure three different graphs are presented: the top one for the sensor at the pulpit (Figure 11a), the central one for the sensor under the portico (Figure 11b), and the lower one for the meteorological station (Figure 11c). The blue lines represent the number of days during which the micropores were saturated all day long, the red one is for days when micropores were saturated only sometimes, and finally, the green line represents days with micropores never being saturated.

Table 7 summarizes the minimum radii of micropores that were never saturated for the whole chosen period. The ratios between the indoor minimum radii and the same evaluated using the meteorological station data were computed.

Inside the church, the values were very similar, around  $5.5 \times 10^{-9}$  m, while under the portico, the minimum radius increased up to around  $3 \times 10^{-8}$  m, and finally at the meteorological station, the value reached  $1.2 \times 10^{-7}$  m. The minimum radius of never-filled micropores can, therefore, be used as a reference to distinguish between indoor and outdoor environments, as the radii change in order of magnitude between indoors and outdoors.

**Table 7.** Minimum radii of never-saturated micropores and the ratio between the indoor and minimum radii.

Locations	Radius (m)	Indoor/Outdoor Ratio
Case (left)	$5.1 \times 10^{-9}$ m	0.042
Case (right)	$5.1 \times 10^{-9}$ m	0.042
Crucifix (bottom)	$5.2 \times 10^{-9}$ m	0.043
Crucifix (top)	$5.3 \times 10^{-9}$ m	0.044
Balustrade (left)	$5.5 \times 10^{-9}$ m	0.045
Balustrade (right)	$5.2 \times 10^{-9}$ m	0.043
Pulpit	$5.3 \times 10^{-9}$ m	0.044
Choir	$5.9 \times 10^{-9}$ m	0.044
Portico	$2.9 \times 10^{-8}$ m	0.239
Meteorological station	$1.2 \times 10^{-7}$ m	1



**Figure 11.** Number of days of saturated micropores as a function of their radii in pulpit (a), portico (b), and meteorological station (c). Blue, red, and green represent the number of days with always, sometimes, and never-saturated micropores, respectively.



#### 4.5. Final Remarks About Microclimatic Indexes

The microclimatic indexes used in this analysis and described in Section 2.3 present different characteristics, as summarized in Table 8. Most indexes use both temperature and relative humidity in their formulas. However, the *NDR* considers only temperature, while the *RH<sub>ratio</sub>* accounts solely for relative humidity. Using only one microclimatic variable can be a disadvantage, as more quantities can better evaluate the microclimate. Moreover, the *IME*, *IMV*, and *NDR* use daily excursions of the physical quantities, while the minimum radius of unfilled micropores and the *PI* use instantaneous values, and finally, the *RH<sub>ratio</sub>* uses both the instantaneous values and a monthly average of the data. Instantaneous values can better describe the situation in real time, but works of art are more vulnerable to large daily excursions of microclimatic variables. Finally, the *PI* and *IME* indexes are defined based on threshold values. The disadvantage of thresholds lies in their fixed values, which do not take into account the historical climate where the work of art of is acclimatized and limited coverage of only one type of artwork, whether chosen by curators or derived from standards (e.g., the UNI10829 [16]).

According to the analysis of the indexes applied to the data of the church of San Panfilo (summarized on the right side of Table 8), it can be concluded that all of them differentiate between indoor and outdoor environments, as their values range greatly. However, differences between indoor locations can only be distinguished by the *IME*, *IMV*, and *NDR*. Indeed, these three indexes show that the microclimatic environments near the crucifix and the pulpit are better than those in other sites within the church.

**Table 8.** Summary of indexes applied to the analysis with their main characteristics.

Indexes	Physical Quantities		Thresholds	Type of Datum	Indoor/ Outdoor	Distinguish Indoor Sites
	Temperature	Relative Humidity				
<i>PI</i>	yes	yes	yes	instant values	yes	no
<i>IME</i>	yes	yes	yes	daily excursions	yes	yes
<i>IMV</i>	yes	yes	no	daily excursions	yes	yes
<i>NDR</i>	yes	no	no	daily excursions	yes	yes
<i>RH<sub>ratio</sub></i>	no	yes	no	instant value and monthly average	yes	no
Minimum radius of unfilled micropores	yes	yes	no	instant values	yes	no

## 5. Conclusions

Indoor microclimatic conditions are affected by outdoor conditions, by the physical properties of the building—mainly its thermal capacity and its absorbing humidity power—and by internal sources (e.g., heating and lighting systems and the presence of people). This work aims to evaluate the influence of the building on environmental conditions by considering some microclimatic indexes.

In this work, we considered a microclimatic campaign that was performed at the parish church of San Panfilo in Tornimparte (L'Aquila, Italy), which is an ancient and massive building hosting an important pictorial cycle of Saturnino Gatti (1494). The internal conditions were measured at some sites by several thermo-hygrometers inside the church; the near-building conditions were measured under the external portico at the main facade, and the outdoor conditions were measured at the nearest meteorological station at Colle San Vito. In the church, the heating system was turned off, and the influence of people and the lighting system was limited [39].

As expected, the time series of temperature measured inside the church was found to be delayed compared to those series near the building and outdoors. In the case study, the temporal delays were three days between indoors and outdoors, while the temperature delay between the measures under the portico and those at the meteorological station was

only two hours. These values can be used as reference parameters in characterizing the influence of the building in microclimatic conditions.

The microclimatic indexes  $PI$ ,  $IME$ ,  $IMV$ ,  $NDR$ , and  $RH_{ratio}$  have been computed for the case study. The results show that all the indexes can distinguish indoor/outdoor conditions, with values lying in different ranges. In particular, considering the  $IMV$  values, the difference in the index between the pulpit site and under the portico site was 0.80 and between the portico site and the meteorological station site was 0.75, resulting in 1.55 between the pulpit site and meteorological station site. The influence of buildings on microclimatic conditions can be compared using these values as a reference.

Based on the results, the indexes are closer in range when evaluating different sites of the church. However, it can be observed that some indexes, namely the  $IME$ ,  $IMV$ , and  $NDR$ , are sensitive to the different conditions inside the church. In fact, they highlighted better microclimatic conditions for the crucifix and the pulpit sites time series measurements that were not affected by the influence of direct radiation on the sensors. Their definitions do not consider daily averages, and their values are dependent on instantaneous measurements. On the contrary, the  $PI$  and  $RH_{ratio}$  can only distinguish between indoor and outdoor conditions, as they consider average values. Among the indexes, the  $IMV$  seems to describe better the microclimatic conditions, as it is defined using both temperature and relative humidity and does not depend on the thresholds based on the standards or the curators' experience.

The evaluation of the minimum radius of never-filled micropores can be used to distinguish between outdoors and indoors, as the radii are different in magnitude. However, the radii of different sites in the church present values that are too close to each other to determine variation indoors.

This study was performed using the data collected in a massive ancient building with thick walls. The findings may have similar implications for similar historic buildings and provide a framework for future studies in microclimate analysis. Therefore, it could be interesting to investigate the application of the same method of analysis to buildings with different thermal capacities to observe the differences and better characterize the influence of the building on microclimatic parameters. Moreover, as the indexes demonstrated that they can distinguish between indoor and outdoor conditions, we propose to include them in future microclimatic operative reports.

**Author Contributions:** Conceptualization, E.R., D.B., and S.F.; methodology, E.R. and S.F.; software, E.R., D.B., and S.F.; validation, E.R. and S.F.; formal analysis, E.R.; investigation, E.R., D.B., and S.F.; resources, D.B.; data curation, D.B.; writing—original draft preparation, E.R.; writing—review and editing, E.R., D.B., and S.F.; visualization, E.R.; supervision, S.F.; project administration, S.F. All authors have read and agreed to the published version of the manuscript.

**Funding:** This research received no external funding.

**Institutional Review Board Statement:** Not applicable.

**Informed Consent Statement:** Not applicable.

**Data Availability Statement:** The data that support the findings of this study are not public; however, they are available for scientific purposes from the corresponding author.

**Acknowledgments:** The authors thank the Pro Loco and the municipality of Tornimparte, the church of San Panfilo for the collaboration, the Italian Association of Archaeometry (AIAR), which organized the measurement campaign between 2021 and 2022, and the Centro Funzionale and Ufficio Idrografico of Regione Abruzzo for the availability of the dataset collected at the meteorological station of Colle San Vito.

**Conflicts of Interest:** The authors declare no conflicts of interest.

## Abbreviations

The following abbreviations are used in this manuscript:

AIAr	Italian Association of Archaeometry
IME	Index of Microclimatic Excursion
IMV	Index of Microclimatic Variabilit
NDR	Normalized Diurnal Range
PI	Performance Index
$RH_{ratio}$	Relative Humidity Ratio

## References

- Camuffo D. *Microclimate for Cultural Heritage*, 3rd ed.; Elsevier: Amsterdam, The Netherlands, 2019; pp. 1–552.
- Bernardi A. *Microclimate Inside Cultural Heritage Buildings*; Ed Il Prato: Padova, Italy, 2008; pp. 1–171.
- Varas-Muriel, M.J.; Fort, R.; Martínez-Garrido, M.I.; Zornoza-Indart, A.; López-Arce, P. Fluctuations in the indoor environment in Spanish rural churches and their effects on heritage conservation: Hygro-thermal and CO<sub>2</sub> conditions monitoring. *Build. Environ.* **2014**, *82*, 97–109. [[CrossRef](#)]
- Sileo, M.; Gizzi, F.T.; Masini, N. Low cost monitoring approach for the conservation of frescoes: The crypt of St. Francesco d’Assisi in Irsina (Basilicata, Southern Italy). *J. Cult. Herit.* **2017**, *23*, 89–99. [[CrossRef](#)]
- Aste, N.; Adhikari, R.S.; Buzzetti, M.; Della Torre, S.; Del Pero, C.; Huerto-Cardenas, H.E.; Leonforte, F. Microclimatic monitoring of the Duomo (Milan Cathedral): Risks-based analysis for the conservation of its cultural heritage. *Build. Environ.* **2019**, *148*, 240–257. [[CrossRef](#)]
- Cataldo, R.; De Donno, A.; De Nunzio, G.; Leucci, G.; Nuzzo, L.; Siviero, S. Integrated methods for analysis of deterioration of cultural heritage: The Crypt of “Cattedrale di Otranto”. *J. Cult. Herit.* **2019**, *6*, 29–38. [[CrossRef](#)]
- Aparicio-Fernández, C.; Vivanco J.L.; Perez-Andreu, V.; Molines-Cano, H.M. Impact of human activity on the thermal behaviour of an unheated church. *Case Stud. Therm. Eng.* **2021**, *28*, 101599. [[CrossRef](#)]
- Corominas i Tabares, J.; Fonseca i Casas, A.; Fonseca i Casas, P. Contribution of Thermal Inertia to the Interior Climate of Girona Cathedral: Feasibility Analysis for the Preservation of Pieces of Art through the Monitoring of Thermal Conditions for 6 Years. *Energies* **2022**, *15*, 1571. [[CrossRef](#)]
- Tringa, E.; Kavrouidakis, D.; Tolika, K. Microclimate-Monitoring: Examining the Indoor Environment of Greek Museums and Historical Buildings in the Face of Clim Change. *Heritage* **2024**, *7*, 1400–1418. [[CrossRef](#)]
- Silva, H.E.; Coelho, G.B.A.; Henriques, F.M.A. Climate monitoring in World Heritage List buildings with low-cost data loggers: The case of the Jerónimos Monastery in Lisbon (Portugal). *J. Build. Eng.* **2020**, *28*, 101029. [[CrossRef](#)]
- Sciurpi, F.; Carletti, C.; Cellai, G.; Pierangioli, L. Environmental Monitoring and Microclimatic Control Strategies in “La Specola” Museum of Florence. *Energy Build.* **2015**, *95*, 190–201. [[CrossRef](#)]
- Andretta, M.; Coppola, F.; Seccia, L. Investigation on the interaction between the outdoor environment and the indoor microclimate of a historical library. *J. Cult. Herit.* **2016**, *17*, 75–86. [[CrossRef](#)]
- Nawalany, G.; Sokółowski, P.; Michalik, M. Experimental Study of Thermal and Humidity Conditions in a Historic Wooden Building in Southern Poland. *Buildings* **2020**, *10*, 118. [[CrossRef](#)]
- Varas-Muriel, M.J.; Fort, R. Microclimatic monitoring in an historic church fitted with modern heating: Implications for the preventive conservation of its cultural heritage. *Build. Environ.* **2018**, *145*, 290–307. [[CrossRef](#)]
- Poljak, M.; Ponechal, R. Microclimatic Monitoring—The Beginning of Saving Historical Sacral Buildings in Europe. *Energies* **2023**, *16*, 1156. [[CrossRef](#)]
- UNI10829; Works of Art of Historical Importance—Ambient Conditions for the Conservation-Measurements and Analysis. UNI Standard Ente Nazionale Italiano di Unificazione: Milano, Italy, 1999; pp. 1–20.
- EN15757; Conservation of Cultural Property-Specifications for Temperature and Relative Humidity to Limit Climate-Induced Mechanical Damage in Organic Hygroscopic Materials. UNE-EN, AENOR: Madrid, Spain, 2010.
- Ilieş, D.C.; Marcu, F.; Caciora, T.; Indrie, L.; Ilieş, A.; Albu, A.; Costea, M.; Burtă, L.; Baias, S.; Ilieş, M.; et al. Investigations of Museum Indoor Microclimate and Air Quality. Case Study from Romania. *Atmosphere* **2021**, *12*, 286. [[CrossRef](#)]
- Corgnati, S.P.; Filippi, M.; Perino, M. A new approach for the IEQ (Indoor Environment Quality) assessment, research in building physics and building engineering. In Proceeding of the 3rd International Conference on Research in Building Physics IBPC 2006, Montreal, QC, Canada, 27–31 August 2006.
- Corgnati, S.P.; Fabi, V.; Filippi, M. A methodology for microclimatic quality evaluation in museums: Application to a temporary exhibit. *Build. Environ.* **2009**, *44*, 1253–1260. [[CrossRef](#)]
- Corgnati, S.P.; Filippi, M. Assessment of thermo-hygrometric quality in museums: Method and in-field application to the “Duccio Di Buoninsegna” exhibition at Santa Maria della Scala (Siena, Italy). *J. Cult. Herit.* **2010**, *11*, 345–349. [[CrossRef](#)]
- Ferdyn-Grygierek, J.; Kaczmarczyk, J.; Blaszczyk, M.; Lubina, P.; Koper, P.; Bulińska, A. Hygrothermal Risk in Museum Buildings Located in Moderate Climate. *Energies* **2020**, *13*, 344. [[CrossRef](#)]
- Huerto-Cardenas, H.E.; Aste, N.; Del Pero, C.; Della Torre, S.; Leonforte, F.; Blavier, C.L.S. Effects of Visitor Influx on the Indoor Climate of the Milan Cathedral. *Atmosphere* **2023**, *14*, 743. [[CrossRef](#)]

24. Schito, E.; Testi, D.; Grassi, W. A Proposal for New Microclimate Indexes for the Evaluation of Indoor Air Quality in Museums. *Buildings* **2016**, *4*, 41–1–41–15. [[CrossRef](#)]
25. Ferrarese, S.; Bertoni, D.; Dentis, V.; Gena, L.; Leone, M.; Rinaudo, M. Microclimatic analysis in the Museum of Physics, University of Turin, Italy: A case-study. *Eur. Phys. J. Plus* **2018**, *133*, 538–1–538–11. [[CrossRef](#)]
26. Lucero-Gómez, P.; Balliana, E.; Farinelli, V.; Salvini, S.; Signorelli, L.; Zendri, E. Rethinking and evaluating the role of historical buildings in the preservation of fragile artworks: The case study of the Gallerie dell'Accademia in Venice. *Eur. Phys. J. Plus* **2022**, *137*, 150–1–150–16. [[CrossRef](#)]
27. Ferrarese, S.; Bertoni, D.; Golzio, A. An index for the evaluation of microclimatic conditions inside museum showcases. *Eur. Phys. J. Plus* **2022**, *137*, 1376–1–1376–9. [[CrossRef](#)]
28. Camuffo, D.; della Valle, A.; Bertolin, C.; Santorelli, E. Temperature observations in Bologna, Italy, from 1715 to 1815: A comparison with other contemporary series and an overview of three centuries of changing climate. *Clim. Chang.* **2017**, *142*, 7–22. [[CrossRef](#)]
29. Verticchio, E.; Frasca, F.; Bertolin, C.; Siani, A.M. Climate-induced risk for the preservation of paper collections: Comparative study among three historic libraries in Italy. *Build. Environ.* **2021**, *206*, 108394–1–108394–16. [[CrossRef](#)]
30. Camuffo, D.; Sturaro, G.; Valentino, A. Urban Climatology Applied to the Deterioration of the Pisa Leaning Tower, Italy. *Theor. Appl. Climatol.* **1999**, *63*, 223–231. [[CrossRef](#)]
31. Camuffo, D.; Sturaro, G.; Valentino, A. Thermodynamic exchanges between the external boundary layer and the indoor microclimate at the Basilica of Santa Maria Maggiore, Rome, Italy: The problem of conservation of ancient works of art. *Bound.-Lay. Meteorol.* **1999**, *92*, 243–262. [[CrossRef](#)]
32. Bernardi, A.; Todorov, V.; Hristova, J. Microclimatic analysis in St. Stephan's church, Nessebar, Bulgaria after interventions for the conservation of frescoes. *J. Cult. Herit.* **2000**, *1*, 281–286. [[CrossRef](#)]
33. Galli, A.; Alberghina, M.F.; Re, A.; Magrini, D.; Grifa, C.; Ponterio, R.C.; La Russa, M.F. Special Issue: Results of the II National Research Project of AIAR: Archaeometric Study of the Frescoes by Saturnino Gatti and Workshop at the Church of San Panfilo in Tornimparte (AQ, Italy). *Appl. Sci.* **2023**, *13*, 8924–1–8924–13. [[CrossRef](#)]
34. Germinario, L.; Giannossa, L.C.; Lezzerini, M.; Mangone, A.; Mazzoli, C.; Pagnotta, S.; Spampinato, M.; Zoleo, A.; Eramo, G. Petrographic and Chemical Characterization of the Frescoes by Saturnino Gatti (Central Italy, 15th Century). *Appl. Sci.* **2023**, *13*, 7223. [[CrossRef](#)]
35. Andreotti, A.; Izzo, F.C.; Bonaduce, I. Archaeometric Study of the Mural Paintings by Saturnino Gatti and Workshop in the Church of San Panfilo, Tornimparte (AQ): The Study of Organic Materials in Original and Restored Areas. *Appl. Sci.* **2023**, *13*, 7153. [[CrossRef](#)]
36. Armetta, F.; Giuffrida, D.; Ponterio, R.C.; Martinez, M.F.F.; Briani, F.; Pecchioni, E.; Santo, A.P.; Ciaramitaro, V.C.; Saladino, M.L. Looking for the Original Materials and Evidence of Restoration at the Vault of the San Panfilo Church in Tornimparte (AQ). *Appl. Sci.* **2023**, *13*, 7088. [[CrossRef](#)]
37. Calandra, S.; Centauro, I.; Laureti, S.; Ricci, M.; Salvatici, T.; Sfarra, S. Application of Sonic, Hygrometric Tests and Infrared Thermography for Diagnostic Investigations of Wall Paintings in St. Panfilo's Church. *Appl. Sci.* **2023**, *13*, 7026. [[CrossRef](#)]
38. Bonizzoni, L.; Caglio, S.; Galli, A.; Lanteri, L.; Pelosi, C. Materials and Technique: The First Look at Saturnino Gatti. *Appl. Sci.* **2023**, *13*, 6842. [[CrossRef](#)]
39. Ferrarese, S.; Bertoni, D.; Golzio, A.; Lanteri, L.; Pelosi, C.; Re, A. Indoor Microclimate Analysis of the San Panfilo Church in Tornimparte, Italy. *Appl. Sci.* **2023**, *13*, 6770–1–6770–17. [[CrossRef](#)]
40. Bonizzoni, L.; Caglio, S.; Galli, A.; Germinario, C.; Izzo, F.; Magrini, D. Identifying Original and Restoration Materials through Spectroscopic Analyses on Saturnino Gatti Mural Paintings: How Far a Noninvasive Approach Can Go. *Appl. Sci.* **2023**, *13*, 6638. [[CrossRef](#)]
41. Comite, V.; Bergomi, A.; Lombardi, C.A.; Borelli, M.; Fermo, P. Characterization of Soluble Salts on the Frescoes by Saturnino Gatti in the Church of San Panfilo in Villagrande di Tornimparte (L'Aquila). *Appl. Sci.* **2023**, *13*, 6623. [[CrossRef](#)]
42. Briani, F.; Caridi, F.; Ferella, F.; Gueli, A.M.; Marchegiani, F.; Nisi, S.; Paladini, G.; Pecchioni, E.; Politi, G.; Santo, A.P.; et al. Multi-Technique Characterization of Painting Drawings of the Pictorial Cycle at the San Panfilo Church in Tornimparte (AQ). *Appl. Sci.* **2023**, *13*, 6492. [[CrossRef](#)]
43. Lanteri, L.; Calandra, S.; Briani, F.; Germinario, C.; Izzo, F.; Pagano, S.; Pelosi, C.; Santo, A.P. 3D Photogrammetric Survey, Raking Light Photography and Mapping of Degradation Phenomena of the Early Renaissance Wall Paintings by Saturnino Gatti—Case Study of the St. Panfilo Church in Tornimparte (L'Aquila, Italy). *Appl. Sci.* **2023**, *13*, 5689. [[CrossRef](#)]
44. Thomson, W. (Lord Kelvin) On the Equilibrium of Vapour at a Curved Surface of Liquid. *Proc. R. Soc. Edinb.* **1870**, *7*, 63–69. [[CrossRef](#)]
45. Bolton, D. The computation of equivalent potential temperature. *Mon. Weather Rev.* **1980**, *108*, 1046–1053. [[CrossRef](#)]

**Disclaimer/Publisher's Note:** The statements, opinions and data contained in all publications are solely those of the individual author(s) and contributor(s) and not of MDPI and/or the editor(s). MDPI and/or the editor(s) disclaim responsibility for any injury to people or property resulting from any ideas, methods, instructions or products referred to in the content.